BIOCHEMISTRY
including biophysical chemistry & molecular biology
Article

Biochemistry **2009,** *48,* 5483–5491 5483
DOI: 10.1021/bi900385g

Synthesis of Nitric Oxide by the NOS-like Protein from *Deinococcus radiodurans*: A Direct Role for Tetrahydrofolate†

Steven Y. Reece,‡ Joshua J. Woodward,§ and Michael A. Marletta*,‡,§,∥,⊥

§*Department of Chemistry and* ⊥*Department of Molecular and Cell Biology and* ‡*California Institute for Quantitative Biosciences and* ∥*Division of Physical Biosciences, Lawrence Berkeley National Laboratory, University of California, Berkeley, California 94720-3220*

Received March 6, 2009; Revised Manuscript Received April 22, 2009

ABSTRACT: Genes encoding for proteins with high sequence homology to the heme-containing, oxygenase domain of mammalian nitric oxide synthase (NOS) have been identified in a number of bacteria. Many of these species of bacteria do not contain the genes that encode for the synthetic machinery to produce tetrahydrobiopterin (H_4B), a cofactor of NOS required for NO synthesis. These bacteria have the genes for the synthesis of tetrahydrofolate (H_4F) which contains the redox-active pteridine ring of H_4B. These observations led us to investigate whether H_4F could be used for the synthesis of NO by NOS-like enzymes from bacteria that cannot make H_4B. The NOS gene from one such bacterium, *Deinococcus radiodurans*, was cloned and expressed (deiNOS) in *Escherichia coli* and then purified and characterized. The K_D of deiNOS for the NOS substrate arginine (0.9 ± 0.1 mM) drops by over 2 orders of magnitude in the presence of H_4F (7.4 ± 0.1 μM). Further, NO is synthesized from the NOS substrate *N*-hydroxy-L-arginine (NHA) by deiNOS in the presence of H_4F. Stopped-flow spectroscopic data reveal that H_4F accelerates the rate of decay of the ferrous−oxy/ferric−superoxo species in substrate turnover. These data strongly suggest that H_4F may be used by *D. radiodurans* to replace H_4B as a redox-active cofactor for nitric oxide synthesis.

Nitric oxide synthase (NOS)[1] catalyzes the synthesis of nitric oxide (NO) and citrulline from L-arginine, molecular oxygen, and NADPH (Scheme 1) (*1*). NO plays a prominent role in mammals in the host response to infection (*2*) and as a signaling molecule involved in neurotransmission, in regulation of blood flow in the vascular system, and in the function of many organs and tissues (*1*, *3*, *4*). NOS from eukaryotes is comprised of an N-terminal oxygenase domain containing cysteine-ligated heme and tetrahydrobiopterin (H_4B) cofactors, a C-terminal reductase domain that binds flavin mononucleotide (FMN) and flavin adenine dinucleotide (FAD), and an intervening calmodulin binding region (*5*). The chemistry of NOS occurs in two mechanistically distinct steps with *N*-hydroxy-L-arginine (NHA) as a stable intermediate (*6*). In both steps, oxygen binds to the ferrous heme and is activated for the subsequent chemistry by electron transfer from the reductase domain and the proximal H_4B (*7*, *8*). Electron transfer from the pterin cofactor to the heme is the rate-limiting step for both Arg and NHA oxidation in single-turnover experiments (*9*).

Recently, a number of species of bacteria have been identified with NOS-like enzymes in their genome (*10*−*15*). Most of these so-called bacterial NOS enzymes are comprised of a single domain with high sequence homology to the oxygenase domain of mammalian NOS. Interestingly, all of the bacterial species that, to date, have been shown to make NO via an NOS-dependent mechanism (*16*, *17*) also contain the genes for H_4B. The biosynthesis of H_4B from GTP occurs via a multistep process involving GTP cyclohydrolase I, 6-pyruvoyltetrahydropterin synthase, and sepiapterin reductase (*18*, *19*). Another NOS-like enzyme from *Bacillus subtilis* (bsNOS) has been shown to produce NO *in vitro*, and this bacterium also contains the genes encoding for the biosynthesis of H_4B (*20*).

Other prokaryotes exist which contain genes encoding for NOS-like proteins but lack the genes for H_4B synthetic machinery. One such bacterium is *Deinococcus radiodurans*, which is remarkable for its extreme radiation resistance (*21*). The gene for NOS in *D. radiodurans* has been cloned and the protein (deiNOS) expressed in *Escherichia coli*, purified, and reported to produce nitrite *in vitro* in the presence of arginine and an oxidation agent in the form of hydrogen peroxide alone or oxygen reduced with equivalents from NADH and the human iNOS reductase domain (*22*, *23*). In addition, when the reaction was supplemented with tryptophan, 4-nitrotryptophan was detected as a product. Trp was suggested to perform the function of H_4B in mammalian

†Funding was provided by the Aldo DeBenedictis Fund.

*To whom correspondence should be addressed at the QB3 Institute, 570 Stanley Hall, University of California, Berkeley. Telephone: (510) 666-2766. Fax: (510) 666-2765. E-mail: marletta@berkeley.edu.

[1]Abbreviations: ALA, 5-aminolevulinic acid hydrochloride; Arg, L-arginine; H_2F, 7,8-dihydrofolic acid; iNOS, full-length inducible nitric oxide synthase; $iNOS_{heme}$, heme domain of inducible nitric oxide synthase; NHA, *N*-hydroxy-L-arginine; NO, nitric oxide; NOS, nitric oxide synthase; deiNOS, nitric oxide synthase-like protein from *Deinococcus radiodurans*; H_4B, (6*R*)-5,6,7,8-tetrahydro-L-biopterin dihydrochloride; H_4F, (6*S*)-5,6,7,8-tetrahydrofolic acid; Trp, tryptophan; 4-NO_2W, 4-nitrotryptophan; NDA, 2,3-naphthalenedicarboxaldehyde; NOA, nitric oxide analyzer; MeCN, acetonitrile.

 Published on Web 04/23/2009

Scheme 1: Reactions Catalyzed by Nitric Oxide Synthase (NOS)

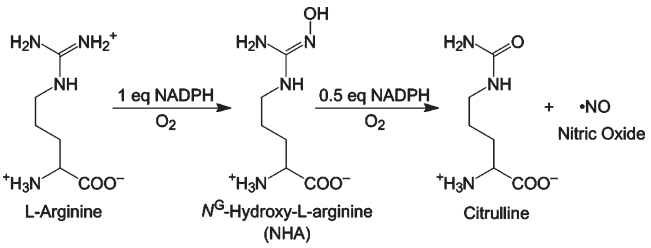

Chart 1: Chemical Structures of H_4F and H_4B

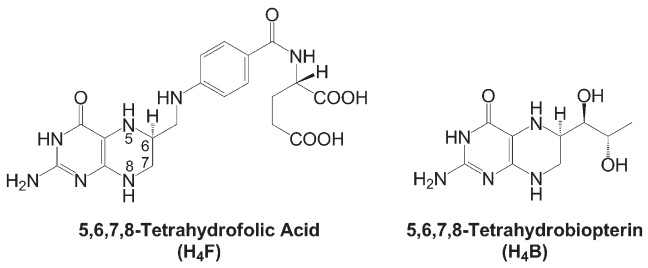

NOS catalysis, in that it may provide a necessary electron for oxygen activation and become regiospecifically nitrated in the process (*23*). This proposed mechanism of 4-NO_2-Trp production was linked to the production of thaxtomin, a dipeptide plant phytotoxin responsible for the pathogenicity of *Streptomyces turgidiscabies* (*24*), as thaxtomin also contains the 4-NO_2-Trp moiety. More recent work with *Streptomyces* NO production, Trp nitration, and thaxtomin production raises questions about the nitration chemistry. Although *Streptomyces* NOS was responsible for cellular NO, the rate of NO production far exceeded the rate of thaxtomin synthesis, thus suggesting an alternative mechanism for peptide nitration (*16*).

Since *D. radiodurans* lacks the enzymes for H_4B biosynthesis and the function of this enzyme remains unclear, we became interested in investigating the *in vitro* biochemistry of deiNOS. Tetrahydrofolate (H_4F) is another prevalent biological molecule that contains the pteridine ring responsible for the redox function of H_4B in NO biosynthesis (Chart 1). H_4F is synthesized *in vivo* from dihydropteroate diphosphate and *p*-aminobenzoic acid in a multistep reaction requiring dihydropteroate synthetase, dihydrofolate synthase, and dihydrofolate reductase (*25*, *26*). The *D. radiodurans* genome contains genes that encode for these proteins (*10*). Recent X-ray structural (*27*) and solution reactivity (*20*) work has suggested that H_4F may replace H_4B in bacterial NOS catalysis. For deiNOS, H_4F (along with H_4B) was shown to support nitrite formation in the presence of NHA, calmodulin, oxygen, NADPH, and the reductase domain of nNOS with an apparent K_M of 20 μM (*22*).

Reported here is a detailed characterization with mechanistic studies of deiNOS. Solution titrations show that H_4F does indeed bind to deiNOS and binding of H_4F reduces the K_D of the enzyme for arginine by an order of magnitude. Single-turnover product analysis reveals, for the first time, that the Fe(II)-containing, deiNOS:H_4F does indeed react with oxygen and NHA to produce NO and citrulline. Stopped-flow data show that H_4F accelerates the decay of Fe(II)$-O_2$ in the presence of Arg or NHA, as opposed to H_2F, and implicates H_4F directly as a coreactant in deiNOS catalysis. Tryptophan, in contrast, does not support NO formation from NHA. These data combined suggest that H_4F may replace H_4B in NOS from bacteria that cannot produce H_4B, thus suggesting a new function for H_4F: as a redox-active cofactor for NO biosynthesis.

MATERIALS AND METHODS

Materials. Dithionite, 4-nitroindole, tris(hydroxymethyl) aminomethane (Tris), trifluoroacetic acid (TFA), 2-mercaptoethanol, ethylenediaminetetraacetic acid (EDTA), chymostatin, pepstatin, leupeptin, antipain, deoxyribonuclease I (DNase I), pyridoxal 5′-phosphate hydrate (PLP), ammonium sulfate, sodium azide (NaN_3) (Sigma-Aldrich), dimethyl sulfoxide (DMSO), glycerol, sodium chloride (Fisher), L-tryptophan, L-arginine hydrochloride, 2,3-naphthalenedicarboxaldehyde (NDA) (Fluka), Luria broth (LB), terrific broth (TB), 4-(2-hydroxyethyl)-1-piperazineethanesulfonic acid (HEPES), dithiothreitol (DTT), ampicillin, kanamycin monosulfate, isopropyl β-D-thiogalactopyranoside (IPTG) (Research Products International (RPI)), Pefabloc SC (pentapharm), L-hydroxyarginine acetate (NHA) (Cayman Chemicals), 5-aminolevulinic acid hydrochloride (ALA) (Cosmo Bio), (6*R*)-5,6,7,8-tetrahydro-L-biopterin dihydrochloride (H_4B), (6*S*)-5,6,7,8-tetrahydrofolic acid (H_4F), and 7,8-dihydrofolic acid (H_2F) (Schircks Laboratories) were used as received. The R1 strain of *D. radiodurans* (ATCC number 13939) and its genomic DNA (ATCC number 13939) were purchased from ATCC, along with the pSTB7 plasmid in *E. coli* encoding for the α and β subunits for tryptophan synthase (TS) (ATCC number 37845). The S219 V mutant of TEV protease with an N-terminal His tag and C-terminal poly-Arg tag was expressed and purified as previously described (*28*). The heme oxygenase domain of murine iNOS ($iNOS_{heme}$) was expressed in *E. coli* and isolated as previously described (*8*).

Spectroscopy. UV−vis spectroscopy was performed on a Cary 3E UV−vis spectrophotometer. ^1H NMR spectra were recorded on a Bruker AV-300 spectrometer in the UC Berkeley College of Chemistry NMR Facility. Mass spectra were recorded on an Agilent 1100 LC/MS equipped with a quadrupole ion detector.

General Methods. H_4B stock solutions (~10 mM) were prepared in 100 mM HEPES, pH 7.5, buffer containing 100 mM DTT, and the concentration was evaluated using ε(297 nm) = 8710 M^{-1} cm^{-1} (*29*). H_4F stocks (~10 mM) were prepared in DMSO containing 100 mM DTT, and the concentration was determined using ε(298 nm) = 28000 M^{-1} cm^{-1} (*30*). H_2F stocks (~10 mM) were prepared in DMSO, and the concentration was evaluated using ε(282 nm) = 28600 M^{-1} cm^{-1} (*31*). Dithionite stock solutions (10 mM) were prepared fresh on the day of the experiment. The sodium hydrosulfite solid was weighed in an Eppendorf vial and brought into an anaerobic glovebag, dissolved in water, and titrated against ferricyanide (ε(420 nm) = 1000 M^{-1} cm^{-1}) in water.

Construction of the deiNOS Expression Vector. The gene encoding for deiNOS was cloned from *D. radiodurans* genomic DNA (ATCC 13939D-5) using the forward (5′ to 3′) primer GGG AAT TCC ATA TGA GTT GCC CCG CTG CCG CC encoding for an *Nde*I restriction enzyme cut site and the reverse (3′ to 5′) primer CGC GGA TCC TTA CCC AGT TGG GGC-ATG encoding for a *Bam*HI restriction enzyme cut site. PCR reactions were carried out in the presence of 2% DMSO using the Expand High Fidelity polymerase enzyme (Roche). The ~1.1 kbp PCR products were purified by electrophoresis on a 1.5%

agarose gel and ligated into a pET28b expression vector encoding for an N-terminal His tag followed by a TEV protease cleavage site using T4 DNA ligase enzyme (New England Biolabs). The pET28b-deiNOS vector construct was transformed into *E. coli* DH5α cells via heat shock and grown on agar plates containing 30 μg/L kanamycin. The DNA from selected colonies were isolated and sequenced by Elim Biopharmaceuticals, Inc. (Hayward, CA).

Expression and Purification of deiNOS. The pET28b-deiNOS vector was transformed into *E. coli* BL21 DE3 cells via heat shock and grown on agar plates containing 30 μg/L kanamycin. A single colony was selected and grown overnight in 60 mL of LB containing 30 μg/L kanamycin. Ten milliliters of this culture was used to inoculate each of six 2 L flasks containing 1 L of TB media and 30 μg/L kanamycin. Bacteria were grown at 37 °C to an $OD_{600nm} \approx 0.6$, at which time IPTG and ALA were added to final concentrations of 1 mM and 450 μM, respectively. The flasks were shaken at 250 rpm for 24 h at room temperature. Cells were harvested by centrifugation at 7000*g* for 20 min, and the pellets were resuspended in buffer A (50 mM HEPES, pH 8.0, 300 mM NaCl, 5 mM Arg, 10 mM imidazole, and 10% glycerol). A cocktail of protease inhibitors containing Pefabloc SC (1 mM), antipain, pepstatin, chymostatin (1 μg/mL), and leupeptin (5 μg/mL) was added along with DNase I (5 μg/mL), the cells were lysed by passage through an EmulsiFlex C-5 homogenizer at 4 °C, and the resulting mixture was centrifuged at 220000*g* for 1 h. The supernatant was then applied to a 30 mL column containing Ni-NTA Superflow resin (Qiagen) that had been previously equilibrated with buffer A at 4 °C. The column was washed with 200 mL of buffer A and 200 mL of buffer A containing 50 mM imidazole. The target protein was eluted with 60 mL of buffer A containing 200 mM imidazole. TEV protease was then added to the deiNOS-containing fraction at a ratio of 1 OD_{280nm} TEV:10 OD_{280nm} deiNOS, and the solution was dialyzed overnight at 4 °C against 2 L of buffer containing buffer B (50 mM HEPES, pH 8.0, 5 mM Arg, 10 mM NaCl, and 10% glycerol). The solution was then passed over another Ni-NTA column that had been equilibrated with buffer B at 4 °C, and deiNOS was eluted with buffer B containing 50 mM imidazole. The enzyme was then concentrated to 100 μM on an Amicon YM-10 membrane; aliquots were frozen in liquid N_2 and stored at −80 °C.

Expression and Purification of Tryptophan Synthase (TS). TS was expressed and purified by a method slightly modified from that previously reported (*32*). Ten milliliters of an overnight culture of *E. coli* containing the pSTB7 plasmid (ATCC number 37845) in Luria broth were used to inoculate each of six 2 L flasks containing 1 L of Vogel and Bonner minimal media (*33*) supplemented with 0.5% glucose, 0.05% acid-hydrolyzed casein, 10 mg/L L-tryptophan, and 30 μg/L ampicillin. The culture was shaken at 250 rpm for 20 h at 37 °C. Cells were harvested by centrifugation at 7000*g* for 20 min, and the pellets were resuspended in 20 mL of buffer C (0.1 M potassium phosphate, pH 7.8, 10 mM 2-mercaptoethanol, 5 mM EDTA, 0.02 mM PLP, and 1 mM Pefabloc SC). The cells were lysed by passage through an EmulsiFlex C-5 homogenizer at 4 °C, and the resulting mixture was centrifuged at 20000*g* for 1 h. Ammonium sulfate (5.31 g) was added to the supernatant (30 mL). The pH was adjusted to 7.5 with concentrated ammonium hydroxide, and upon standing for 30 min at 4 °C, the solution centrifuged for 20 min at 20000*g*. The supernatant was decanted off and the pellet discarded. Ammonium sulfate (2.82 g) was added to the solution, the pH again adjusted to 7.5 with ammonium hydroxide, and upon standing for 30 min at 4 °C, the mixture was centrifuged for 20 min at 20000*g*. The supernatant was discarded and the pellet dissolved in 5 mL of buffer C. This solution was dialyzed overnight in a 10000 MW cutoff dialysis cassette (Thermo-Scientific) against 200 mL of buffer C. The purified protein was assayed as described in ref *32* and exhibited a specific activity of 725 units/mg.

Enzymatic Synthesis of 4-Nitro-L-tryptophan (4-NO_2W). A 1 L Erlenmeyer flask was charged with 500 mL of 100 mM potassium phosphate buffer (pH 8) containing 15 mM serine, 30 μM PLP, 16.2 mM NaCl, and 2 mM NaN_3. 4-Nitroindole (100 mg) in 10 mL of DMSO and 10000 units of tryptophan synthase were then added, and the solution was shaken at 37 °C for 4 days. Another 10000 units of TS was added and the reaction shaken at 37 °C for an additional 4 days. The reaction progress was monitored by HPLC on a Beckman System Gold instrument using 0−65% MeCN gradient over 45 min vs 0.1% formic acid with a NovaPack C_{18} analytical column (3.9 × 150 mm). The substrate eluted with a retention time of 26.8 min, while the product eluted at 12.0 min. The reaction mixture was loaded onto a 200 mL (4 × 17 cm) AG50W-X8 (50−100 mesh) cation-exchange resin, which had previously been washed with 5 column volumes of 1 M NaOH, 5 column volumes of 1 M HCl, and 1 column volume of water. The product was eluted with 1% ammonium hydroxide and the solvent removed *in vacuo* to yield a bright yellow solid (50 mg, 33% yield). ^{1}H NMR (400 MHz, D_2O + NaOD): δ 2.94 (dd, 1H, $C_\beta-H_1$, 6.8 Hz, 14.4 Hz), 3.10 (dd, 1H, $C_\beta-H_2$, 6.4 Hz, 14.2 Hz), 3.22 (t, 1H, $C_\alpha-H$, 6.8 Hz), 7.15 (dd, 1H, aromatic C−H, 7.6 Hz, 8.4 Hz), 7.37 (s, 1H, aromatic C−H), 7.71 (d, 1H, aromatic C−H, 8.0 Hz), 7.79 (d, 1H, aromatic C−H, 7.6 Hz). LR-ESI-MS: m/z $[M + H]^+$ calcd 250.1, obsd 250.3.

Extinction Coefficient for Heme in deiNOS. Analytical HPLC on a Beckman System Gold instrument was used to quantify the amount of heme in deiNOS. Heme stocks were prepared in 2:1 200 mM Na_2HPO_4/100 mM NaOH:DMSO and diluted into 100 mM HEPES buffer (pH 7.5) containing 100 μM bovine serum albumin (BSA) which was added to increase heme solubility. Samples (20 μL) were injected onto a Vydac C_4 protein column (250 × 2 mm) and eluted using 0.1% TFA/H_2O (solvent A) and 0.05% TFA/MeCN (solvent B) with the following gradient: 20% B for 5 min, 20−60% B over 20 min, 60−95% B for 2 min, and 95% B for 5 min. During the run, heme is separated from protein for both the BSA standards and deiNOS sample, as determined by absorption spectrum of free heme in the observed HPLC traces. A calibration curve was generated over the range of 0.5−50 μM heme.

To calculate the extinction coefficient, the absorption spectrum of the Fe(III)−imidazole complex of deiNOS in 100 mM HEPES (pH 7.5) was measured, and the protein solution was injected onto the HPLC for heme quantification. The resulting extinction coefficient for the Soret transition of the ferric−imidazole complex was measured as $\varepsilon(427\text{ nm}) = 97000 \pm 2000\ M^{-1}\ cm^{-1}$.

Analytical Gel Filtration. AGF was performed on the Beckman System Gold HPLC using an Agilent Zorbax GF-250 column (4 μm, 9.4 × 250 mm). The mobile phase was 100 mM HEPES (pH 7.5), 200 mM NaCl, and 5 mM Arg, and the flow rate was 1.0 mL/min. The following standards were used to generate a calibration curve: apoferritin (MW = 443 kDa, t_r = 9.09 min), alcohol dehydrogenase (150 kDa, 10.05 min), bovine

serum albumin (66 kDa, 10.36 min), chicken egg white albumin (45 kDa, 10.98 min), carbonic anhydrase (29 kDa, 11.93 min), and cytochrome *c* (12.3 kDa, 12.91 min). The calculated molecular mass of deiNOS is 40 kDa, and the protein eluted as a single peak with a retention time of 10.60 min (83 kDa) indicating that the protein elutes as a dimer.

Substrate and Cofactor Binding. Arg and NHA binding in the presence and absence of H_4B, H_4F, and Trp was monitored by UV−vis spectroscopy. Protein solutions were prepared in 100 mM HEPES buffer (pH 7.5), and spectra were recorded upon addition of aliquots of substrate. Spectra were corrected for dilution after each addition, and the total change in volume over the titration was less than 10%. The difference spectra were plotted, and K_D was determined by fitting the double difference ($\Delta\Delta A = \Delta A_{max} - \Delta A_{min}$) as a function of substrate concentration to the saturation binding equation: $\Delta\Delta A = (\Delta\Delta A_{max}$ [substrate])/(K_D + [substrate]).

Reactions of deiNOS with Hydrogen Peroxide. Reactions of deiNOS with hydrogen peroxide in the presence of tryptophan and arginine were carried out as previously described (*23*). Trp and 4-NO_2W were separated on a Beckman System Gold HPLC instrument using a 0−30% MeCN gradient over 30 min vs 0.1% formic acid with a NovaPack C_{18} analytical column (3.9 × 150 mm). Trp and 4-NO_2W eluted with retention times of 7.7 and 14.5 min, respectively. deiNOS was desalted on a PD-10 column into buffer containing 50 mM Tris (pH 7.5), 200 mM NaCl, 0.3 M Arg, and 20 mM Trp. The protein was diluted in the same buffer to a final concentration of 50 μM and the reaction initiated with 20 mM H_2O_2. Peroxide concentrations were determined using the reported extinction coefficient, $\varepsilon(240\text{ nm}) = 39.4\text{ M}^{-1}\text{ cm}^{-1}$ (*34*). Vigorous evolution of bubbles from the reaction solution was observed upon addition of peroxide; however, no 4-NO_2W could be observed using the HPLC assay described above.

Amino Acid Product Analysis of Single-Turnover Reactions. Sample preparations were performed in an anaerobic glovebag. Stock solutions of deiNOS were desalted on a Sephadex G-25 M, PD-10 column (GE Healthcare) with 100 mM HEPES (pH 7.5) buffer as the eluant. Heme-containing fractions were pooled and concentrated to ~80 μM using a VivaSpin 500 10 kDa molecular mass cutoff spin concentrator (Sartorius Stedim Biotech). Reaction solutions (50 μL) were prepared in Eppendorf tubes with 50 μM deiNOS, 250 μM H_4B/H_4F, and 1 mM Arg/NHA. Under these conditions, the protein is saturated with substrate and bound cofactor, as determined by UV−vis spectroscopy of the high-spin ferric state. Dithionite was then added to a final concentration of 50 μM (1 equiv) and the solution allowed to stand at room temperature for 10 min. The tubes were removed from the glovebag and exposed to air to initiate the reaction. Phenylalanine (100 μM) was added as an internal standard.

Amino acid products were derivatized with NDA and separated using an Agilent 1200 series HPLC equipped with a NovaPak C_{18} column (150 × 3.9 mm, 4 μm; Waters) and an Altima C_{18}-LL guard column (5 μm; Alltech) with a method slightly modified from that described previously (*8*). The reaction solution (40 μL) was mixed with 18 μL of 50 mM NaCN in 0.1 M potassium borate buffer (pH 9.5) and 9 μL of 10 mM NDA in methanol. The solutions were allowed to stand at room temperature for at least 15 min. Samples were loaded into the HPLC autosampler, and 40 μL of reaction volume was injected onto the reversed-phase column, which was held at 40 °C. Reactions with Arg as the substrate were separated using 5 mM ammonium acetate, 20% methanol (solvent A), and MeCN (solvent B) with a flow rate of 0.7 mL/min and the following gradient: 20% B for 16 min, 20−65% B over 8 min, 65−100% B over 2 min, 100% B for 2 min, 100−20% B over 0.5 min, and 20% B for 6 min. Elution of derivatized amino acids was monitored by absorbance at 421 nm. NHA, Arg, and Phe eluted with retention times of 5.5, 6.2, and 19.9 min, respectively. Reactions with NHA as the substrate were separated using 5 mM ammonium acetate, 20% methanol (solvent A), and methanol (solvent B) with a flow rate of 0.5 mL/min and the following gradient: 0−30% B over 3 min, 30−35% B over 5 min, 35−50% B over 7 min, 50−100% B over 5 min, 100% B for 5 min, 100−0% B over 0.5 min, and 100% A for 5 min. Citrulline, NHA, and Phe eluted with retention times of 10.6, 14.2, and 19.6 min, respectively. Reported values are the average of at least three reactions.

NO Formation from Single-Turnover Reactions. Samples were prepared as described above for the amino acid product analysis. Reaction solutions (50 μL) were prepared and sealed in Reacti-vials with 50 μM deiNOS, 500 μM H_4B/H_4F or 20 mM Trp, and 1 mM Arg/NHA. Dithionite was then added to a final concentration of 50 μM (1 equiv) and the solution allowed to stand at room temperature for 10 min. The samples were removed from the glovebag, and the reaction was initiated by the addition of an equal volume of 100 mM HEPES buffer (pH 7.5) that had been equilibrated with air. The reactions were shaken for 10 s and allowed to stand for 50 s before 200 μL of headspace was injected onto a Sievers 270 nitric oxide analyzer (NOA). The NOA detects NO by reaction with ozone and monitoring the resulting chemiluminescence; thus the signal is highly specific for NO relative to other gaseous nitrogen oxide products (*35*, *36*). The amount of NO produced is reported relative to the amount for an identical reaction containing the heme domain of iNOS (*8*) in place of deiNOS. The values reported are an average of at least three samples.

Stopped-Flow Spectroscopy. Stopped-flow mixing UV−vis spectroscopy was performed using an SF-61 spectrometer (Hi-Tech Scientific). Protein samples (700 μL) containing 5 μM deiNOS, 1 mM Arg/NHA, and 50 μM H_4F/H_2F in 100 mM HEPES buffer (pH 7.5) were prepared in an anaerobic glovebag and allowed to stand at room temperature for 1 h. Binding of substrate and H_4F/H_2F cofactor was verified by UV−vis spectroscopic characterization of high-spin ferric heme. The sample was then reduced with 25 μM dithionite (5 equiv), loaded into an anaerobic syringe, and placed in a T-adapter that contained another syringe with 1 mL of 0.5 mM dithionite. The anaerobic syringes were removed from the glovebag and connected to the spectrometer. The stopped-flow syringe was first scrubbed with the 0.5 mM dithionite solution to remove dissolved oxygen and then loaded with the anaerobic protein sample. The second stopped-flow syringe was loaded with 100 mM HEPES buffer (pH 7.5) that had been saturated with oxygen gas by bubbling on ice for 15 min. Both syringes were allowed to equilibrate at 10 °C prior to injection. Anaerobic protein was mixed with oxygenated buffer in the spectrometer, and absorption spectra were recorded as a function of time. The dead time of mixing was on the order of 1 ms.

Data were baseline corrected and fit from 360 to 680 nm using global fitting software (Specfit version 3.0.14). The data could be appropriately fit to an A → B kinetic model, as observed by the lack of order in the residuals of the fit to the kinetic data. Reported rate constants are the result of this global fitting procedure, and the error is reported as the standard deviation of at least three experiments.

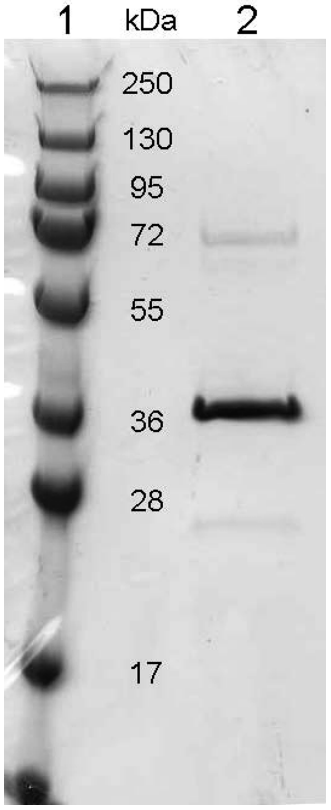

FIGURE 1: SDS−PAGE of purified deiNOS. Lane 1 is a molecular mass marker, and lane 2 contains the purified deiNOS protein.

RESULTS

Cloning, Expression, and Purification of deiNOS. Cloning of the gene encoding for deiNOS and construction of the deiNOS expression vector were carried out using standard procedures with one important exception. The addition of 2% DMSO to the cloning reaction was required for amplification of the deiNOS gene from genomic DNA. For the expression of deiNOS in *E. coli*, the addition of ALA upon induction with IPTG was critical for production of enzyme with optimal heme content. The solubility of deiNOS is greatly increased in the presence of Arg and glycerol; thus the introduction of 5 mM Arg and 10% glycerol in the lysis and purification buffers led to a much larger yield of soluble protein. Figure 1 shows the SDS−PAGE gel of the purified deiNOS protein.

Spectral Characterization of deiNOS and Binding of Substrates and Cofactors. Table 1 lists the spectral transitions of heme in deiNOS in various redox and coordination states. The as-purified enzyme exists as a mixture of high- and low-spin Fe^{3+} when exchanged into 100 mM HEPES buffer (pH 7.5) with λ_{max} = 415 nm. Binding of substrate to iNOS shifts the thermal equilibrium of high/low-spin heme-bound ferric iron to high spin, similar to cytochrome P450 enzymes (*37*). UV−vis spectroscopy serves as a sensitive monitor of this spin state change and thus provides a convenient method for determining binding constants for substrates to NOS (*8*). Figure 2 (top panel) shows the spectra obtained upon titration of a solution of deiNOS with arginine. Most notably, the Soret transition of the heme cofactor shifts from λ_{max} of 413 to 395 nm. Based on the analogous spectral shifts upon titration of $iNOS_{heme}$ with arginine (*8*), this spectral change is attributed to binding of arginine at the active site of deiNOS and the shift of the spin state of heme iron from a mixture of high and low spin to fully high spin. Fitting of the data

Table 1: Spectral Transitions for Various States of Heme in deiNOS

	λ_{max}/nm		
	Soret	α/β	por → Fe CT
Fe^{3+} (as purified)	415	535, 570[a]	646
Fe^{3+} (high spin)	396	512, 547[a]	646
Fe^{3+}−imidazole	427	550, ∼586[a]	∼715
Fe^{2+}	409	535, 555	
Fe^{2+}−imidazole	425	530[a], 555	
Fe^{2+}−CO	446	550, 590[a]	
Fe^{2+}−O_2	420	560, 580[a]	

[a] Shoulder.

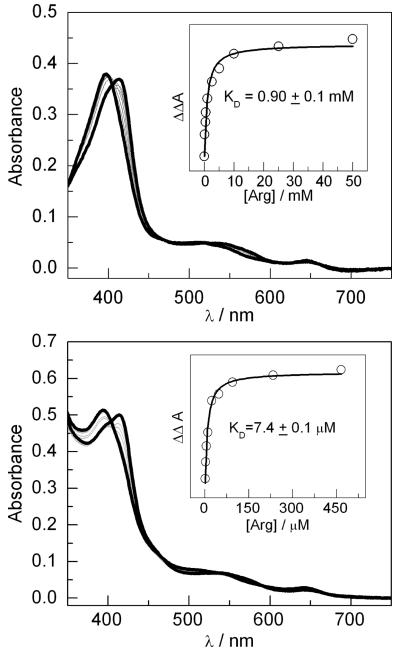

FIGURE 2: Top panel: UV−vis absorption spectra obtained upon titration of deiNOS with Arg. Bottom panel: Same experiment in the presence of 250 μM H_4F. Insets: Plot of $\Delta\Delta A$ as a function of Arg concentration with fit to the saturation binding equation.

to a saturation binding model yields $K_D = 0.9 \pm 0.1$ mM. Similar spectral transitions are observed upon titration of a deiNOS solution containing 250 μM H_4F with arginine (bottom panel). Notably, the K_D for arginine shifts by over 2 orders of magnitude to 7.4 ± 0.1 μM in the presence of 250 μM H_4F. Binding of H_4F was found to be dependent on the concentration of arginine, as seen with $iNOS_{heme}$ (*8*). Incubation of deiNOS with 100 μM arginine and 50 μM H_4F results in a shift in the heme iron spin state to fully high spin. No spectral shifts were observed upon titration of deiNOS with Trp (up to 20 mM Trp). The K_D for Arg in the presence of 500 μM H_4B and 20 mM Trp was measured as 160 and 500 ± 50 μM, respectively.

Figure 3 shows the spectra observed upon reduction of the protein with dithionite and in the presence of CO. Reduction of the protein results in a shift in the Soret band to 409 nm, attributed to the ferrous form of the heme based on analogy to $iNOS_{heme}$ (*8*). Treatment of the reduced protein with CO results in the formation of a narrow Soret band with λ_{max} = 446 nm. This band is similar to the 450 nm transitions formed by the ferrous−CO complexes of cytochrome P450 (*38*, *39*). These

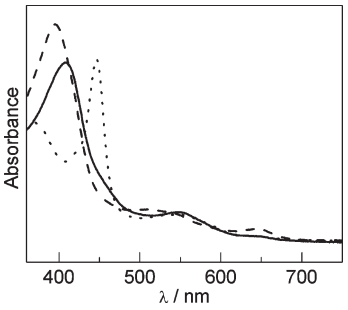

FIGURE 3: UV−vis absorption spectra of solutions of deiNOS in 100 mM HEPES (pH 7.5) containing 50 μM H_4F and 1 mM Arg. The spectra obtained are for the as-purified (Fe^{3+}, high spin, − −), dithionite-treated (Fe^{2+}, —), and dithionite- plus CO-treated (Fe^{2+}−CO, ···) enzyme.

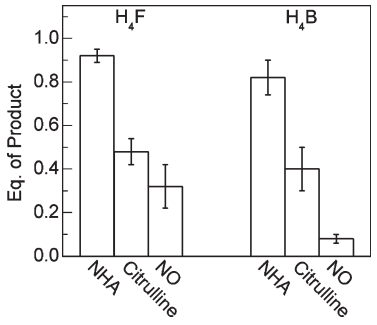

FIGURE 4: Stoichiometry of single-turnover reactions for the production of NHA from Arg and NO plus citrulline from NHA using deiNOS reconstituted with H_4F or H_4B cofactors. Nitric oxide data were obtained with a nitric oxide analyzer, and values are reported using $iNOS_{heme}$ as a reference.

spectral characterization data are similar, but not identical, to that previously reported (*22*).

Reaction Chemistry of deiNOS. Using the HPLC assay described above, reactions of deiNOS with hydrogen peroxide in the presence of tryptophan and arginine did not yield detectable amounts of 4-nitrotryptophan. Single-turnover reactions were carried out by mixing ferric protein with Arg or NHA substrates in the presence of H_4F and H_4B. The protein was reduced by dithionite and then reacted with oxygen to initiate reaction. The results of these reactions are shown in Figure 4 and listed in Table 2. Both H_4F and H_4B support the oxidation of Arg to NHA, with the H_4F-containing reaction proceeding with slightly higher efficiency. Single-turnover arginine oxidation reactions using protein reconstituted with H_4F and H_4B led to the formation of 0.92 ± 0.03 and 0.82 ± 0.08 equiv of NHA, respectively. Similarly, both H_4F and H_4B support the oxidation of NHA to citrulline, with the H_4F-containing reaction proceeding with slightly higher efficiency. Reactions with H_4F- and H_4B-reconstituted protein yielded 0.48 ± 0.06 and 0.40 ± 0.1 equiv of citrulline, respectively. Single-turnover reactions of $iNOS_{heme}$ resulted in similar amounts of citrulline formation (0.65 equiv) when the protein was reduced with 1 equiv of dithionite, as was done here (*8*). In the presence of H_4F, deiNOS produces a similar quantity of NO upon oxidation of NHA as compared to $iNOS_{heme}$. In contrast, H_4B-reconstituted protein produces significantly less NO. NO formation was not observed upon oxidation of deiNOS in the presence of 20 mM Trp and 1 mM NHA (no H_4F or H_4B cofactors).

Kinetics of Turnover. Stopped-flow spectroscopy was used to probe the kinetics of single-turnover reactions of deiNOS.

Table 2: Stoichiometry of Single-Turnover Reactions for deiNOS

	H_4F	H_4B	Trp
Arg + O_2 → NHA + H_2O			
equiv of NHA	0.92 ± 0.03	0.82 ± 0.08	−
NHA + O_2 → Citrulline + H_2O + NO			
equiv of citrulline	0.48 ± 0.06	0.40 ± 0.1	−
equiv of NO[a]	0.3 ± 0.1	0.08 ± 0.02	nd[b]

[a] $iNOS_{heme}$:H_4B was used as a reference, which produces 0.35 equiv of NO under these conditions (*8*). [b] None detected.

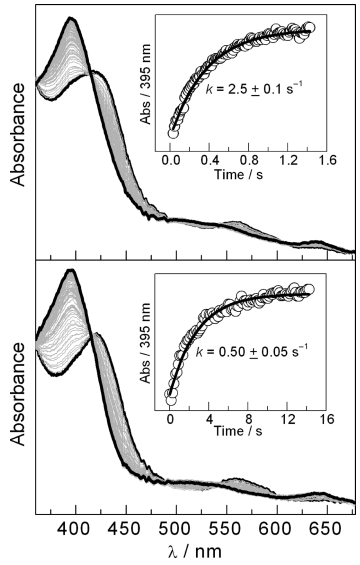

FIGURE 5: Top panel: Stopped-flow spectra measured upon mixing a solution of 5 μM deiNOS, 50 μM H_4F, and 1 mM Arg with oxygenated buffer at 10 °C. Bottom panel: Same experiment, except that 1 mM NHA was used in place of Arg. Insets: Data (○) and single-exponential fit (—) for single-wavelength kinetics observed at 395 nm.

Figure 5 shows the spectra observed upon mixing reduced deiNOS:H_4F with oxygen in the presence of Arg (top) and NHA (bottom). In both of the experiments, the initial species formed had a λ_{max} = 420 nm for the heme Soret transition, which we attribute to the Fe(II)−O_2 species. This species formed within the dead time of the instrument. Table 3 presents the rate constants for decay of this intermediate obtained upon global analysis of these data. The ferrous−oxy species decayed with a rate constant of 2.5 ± 0.1 s^{-1} with Arg as the substrate and 0.5 ± 0.05 s^{-1} with NHA to a spectrum that was identical to that observed for high-spin ferric enzyme. These transitions involve the oxidation of Arg and NHA, respectively, in a manner similar to that reported for $iNOS_{heme}$ (*40*). An important difference, however, is that the Fe(III)−NO species that is usually observed upon oxidation of NHA with $iNOS_{heme}$ was not observed here with deiNOS. When H_2F was used in place of H_4F, identical spectral transitions were observed; however, the reaction was slower (k = 0.10 ± 0.05 s^{-1} for both Arg and NHA substrates).

DISCUSSION

The first characterization of cloned and purified deiNOS reported that deiNOS oxidizes Arg to *nitrite* with H_4B and H_4F cofactors in the presence of hydrogen peroxide or reducing

Table 3: Kinetics for Ferrous−Oxy/Ferric−Superoxo Decay for deiNOS and iNOS

	k/s^{-1}			
	deiNOS:H_4F	deiNOS:H_2F	iNOS:H_4B	iNOS:H_2B
Arg	2.5 ± 0.1	0.1 ± 0.05	12.5 ± 0.2[a]	0.3 ± 0.8[b]
NHA	0.5 ± 0.05	0.1 ± 0.05	36.7 ± 1.1[b]	11.0 ± 0.1[b]

[a] Reference *47*. [b] Reference *45*.

equivalents (NADPH and the reductase domain of neuronal NOS) plus oxygen (*22*). From this work, it was inferred that deiNOS behaves similarly to the oxygenase domain of mammalian NOS in the production of NO from arginine and that H_4F may be used as a cofactor to support NO synthesis in bacteria that lack the enzymes for H_4B biosynthesis. However, nitrite is a common decomposition product of several nitrogen oxides and cannot be equated with nitric oxide formation in NOS assays (*41*).

A subsequent paper reported that the same protein catalyzed the regioselective nitration of Trp at the 4-position (*23*), a reaction that was inhibited by the addition of H_4B. That report suggested that Trp serves the same role as H_4B in mammalian NOS catalysis and donates an electron to the ferrous−oxy/ferric−superoxo species for the activation of oxygen and production of NO (Scheme 2). These results and conclusions are particularly striking given the high reduction potential of $Trp^{\bullet}$ (0.89 V vs NHE, pH 7) (*42*) and the corresponding low thermodynamic driving force for oxidation of Trp by the Fe(III)−O_2^-, ferric−superoxo species. For reference, the reduction potential of the Fe(III)−O_2^- species of cytochrome P450, another thiol-ligated heme-containing oxygenase enzyme, has been estimated at 0.93 V vs NHE, pH 7 (*43*).

We began our investigation of the reactivity of deiNOS by exploring the previously reported Trp nitration reaction (*23*). We determined that tryptophan synthase supports the synthesis of 4-nitro-L-tryptophan (4-NO_2Trp) from 4-nitroinodole and serine, thereby providing a standard with which to compare the reaction products of deiNOS and Trp. Using the conditions reported in ref *23* for reaction of deiNOS with Trp and H_2O_2, along with the HPLC assay described above for separation of 4-NO_2Trp and Trp, 4-nitro-L-tryptophan was not observed as a reaction product.

We investigated the ability of deiNOS to bind typical NOS substrates and potential pterin cofactors, along with its capacity for NO synthesis. As noted above, *D. radiodurans* does not contain the machinery for H_4B formation; however, H_4F also contains the redox-active pterin ring and might possibly substitute for this NOS cofactor in bacteria that cannot synthesize H_4B. The dissociation constant, K_D, of deiNOS for arginine is over 2 orders of magnitude lower upon binding H_4F (900−7.4 μM). A less dramatic shift in the K_D for Arg occurs in the presence of H_4B (160 μM). Both H_4F and H_4B support Arg oxidation to NHA and NHA oxidation to citrulline and nitric oxide. Similar amounts of amino acid products were formed with H_4F and H_4B; however, the amount of NO produced varied depending on the choice of cofactor. For mammalian iNOS, the coupling of citrulline and NO product formation is strongly dependent on the chemical nature of the pterin cofactor (*44*). Importantly, NO was not observed for reaction of reduced deiNOS, NHA, and oxygen with tryptophan as the cofactor. The large shift in the K_D for arginine and the tight coupling of

Scheme 2: Reaction Mechanism for Activation of Oxygen by Tetrahydrobiopterin (H_4B) in NOS[a]

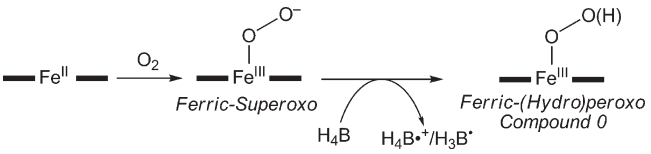

[a] Compound 0 is the fully activated form of oxygen, and it or its decomposition products may react with substrate.

citrulline and NO formation in the presence of H_4F, both of which are reported for the first time in this work, suggest that deiNOS may use H_4F (or a polyglutamated analogue) for NO synthesis *in vivo*. Structural homology models of deiNOS support this hypothesis and predict a strong electrostatic interaction between the negatively charged glutamate side chain of H_4F and a patch of positively charged residues surrounding it at the protein dimer interface (*27*).

Stopped-flow spectroscopy reveals that the rate of decay of the ferrous−oxy/ferric−superoxo species in the presence of oxygen is strongly dependent on the nature of the substrate and the pterin cofactor. Notably, H_4F-reconstituted protein exhibits a 25-fold and 5-fold faster rate of decay with Arg and NHA substrates, respectively, compared to the H_2F-reconstituted analogue. H_2F serves as an approximate structural model of H_4F in binding to deiNOS but lacks the potency as a reducing agent in the activation of oxygen. The enhanced decay kinetics for H_4F compared to H_2F, therefore, suggest that H_4F is a redox-active cofactor that participates directly in Arg and NHA oxidation. Based on the analogous reaction chemistry with H_4B and iNOS (Scheme 2), H_4F would serve to donate an electron to heme in the activation of oxygen. However, several observations distinguish the single-turnover chemistry of deiNOS:H_4F compared to $iNOS_{heme}$:H_4B. The kinetics for ferrous−oxy decay are 5-fold and 73-fold slower for deiNOS:H_4F compared to iNOS:H_4B with Arg and NHA substrates, respectively (Table 3). The decay of the ferrous−oxy/ferric−superoxo species in iNOS:H_4B is kinetically coupled to the formation of a Fe(III)−NO (ferric−nitrosyl) with NHA as the substrate (*45*), while for deiNOS:H_4F decay of the ferrous−oxy species yields high-spin ferric protein. Since the decay of ferrous−oxy in deiNOS:H_4F is rate-limiting, we cannot compare the stability of the Fe(III)−NO species for deiNOS:H_4F and iNOS:H_4B.

The data presented in this report suggest a new role for H_4F in biology. Polyglutamated derivatives of H_4F are widely known as coenzymes in one-carbon metabolism and carry out such reactions as formyl group incorporation into purine rings for the synthesis of formylated methionyl-tRNA in mitochondria, conversion of uridylate into thymidylate, and the methylation of homocysteine to methionine (*46*). We have now unambiguously shown that H_4F can support the *in vitro* synthesis of NO by the nitric oxide synthase-like protein from *D. radiodurans*. Several key observations strongly suggest that H_4F is the natural cofactor for this enzyme *in vivo*. *D. radiodurans* lacks the genes encoding for the synthetic machinery for H_4B, the cofactor required for synthesis of NO in mammalian NOS. H_4F contains the pteridine ring of H_4B that is responsible for its redox-active role in NOS catalysis. *D. radiodurans* does contain the genes encoding for H_4F synthetic machinery. In addition, we have shown that the K_D of deiNOS for the NOS substrate Arg drops by over 2 orders of magnitude upon binding H_4F. Stopped-flow kinetics reveal that

the rate of reaction of the ferrous−oxy/ferric−superoxo species is enhanced upon binding H_4F compared to H_2F. Drawing parallels from the reaction chemistry of iNOS:H_4B, these data suggest a redox-active role for H_4F in the activation of oxygen at heme for nitric oxide synthesis in deiNOS. Experiments are currently underway to enhance our understanding of deiNOS catalysis including attempts to directly observe potential $H_4F^{\bullet+}/H_3F^{\bullet}$ radical intermediates, to identify the degree of glutamation of the natural H_4F cofactor *in vivo*, and to identify the reductase partner of deiNOS in *D. radiodurans*.

ACKNOWLEDGMENT

We acknowledge Prof. Theodor Agapie for providing helpful and stimulating discussions. Mark Price, Lily Chao, and Emily Weinert provided assistance with molecular biology techniques. We also thank the entire Marletta laboratory for careful and critical reading of the manuscript.

REFERENCES

1. Cary, S. P. L., Winger, J. A., Derbyshire, E. R., and Marletta, M. A. (2006) Nitric oxide signaling: No longer simply on or off. *Trends Biochem. Sci. 31*, 231–239.
2. Marletta, M. A., Yoon, P. S., Iyengar, R., Leaf, C. D., and Wishnok, J. S. (1988) Macrophage oxidation of L-arginine to nitrite and nitrate: Nitric oxide is an intermediate. *Biochemistry 27*, 8706–8711.
3. Dawson, V. L., and Dawson, T. M. (1998) Nitric oxide in neurodegeneration. *Prog. Brain Res. 118*, 215–229.
4. Bredt, D. S. (1999) Endogenous nitric oxide synthesis: Biological functions and pathophysiology. *Free Radical Res. 31*, 577–596.
5. Marletta, M. A. (1994) Nitric oxide synthase: Aspects concerning structure and catalysis. *Cell 78*, 927–930.
6. Stuehr, D. J., Kwon, N. S., Nathan, C. F., Griffith, O. W., Feldman, P. L., and Wiseman, J. (1991) N^{ω}-hydroxy-L-arginine is an intermediate in the biosynthesis of nitric oxide from L-arginine. *J. Biol. Chem. 266*, 6259–6263.
7. Hurshman, A. R., Krebs, C., Edmondson, D. E., Huynh, B. H., and Marletta, M. A. (1999) Formation of a pterin radical in the reaction of the heme domain of inducible nitric oxide synthase with oxygen. *Biochemistry 38*, 15689–15696.
8. Hurshman, A. R., and Marletta, M. A. (2002) Reactions catalyzed by the heme domain of inducible nitric oxide synthase: Evidence for the involvement of tetrahydrobiopterin in electron transfer. *Biochemistry 41*, 3439–3456.
9. Wei, C. C., Crane, B. R., and Stuehr, D. J. (2003) Tetrahydrobiopterin radical enzymology. *Chem. Rev. 103*, 2365–2384.
10. White, O., Eisen, J. A., Heidelberg, J. F., Hickey, E. K., Peterson, J. D., Dodson, R. J., Haft, D. H., Gwinn, M. L., Nelson, W. C., Richardson, D. L., Moffat, K. S., Qin, H., Jiang, L., Pamphile, W., Crosby, M., Shen, M., Vamathevan, J. J., Lam, P., McDonald, L., Utterback, T., Zalewski, C., Makarova, K. S., Aravind, L., Daly, M. J., Minton, K. W., Fleischmann, R. D., Ketchum, K. A., Nelson, K. E., Salzberg, S., Smith, H. O., Craig, J., Venter, and Fraser, C. M. (1999) Genome sequence of the radioresistant bacterium *Deinococcus radiodurans* R1. *Science 286*, 1571–1577.
11. Ikeda, H., Ishikawa, J., Hanamoto, A., Shinose, M., Kikuchi, H., Shiba, T., Sakaki, Y., Hattori, M., and Omura, S. (2003) Complete genome sequence and comparative analysis of the industrial microorganism *Streptomyces avermitilis*. *Nat. Biotechnol. 21*, 526–531.
12. Kuroda, M., Ohta, T., Uchiyama, I., Baba, T., Yuzawa, H., Kobayashi, I., Cui, L., Oguchi, A., Aoki, K.-i., Nagai, Y., Lian, J., Ito, T., Kanamori, M., Matsumaru, H., Maruyama, A., Murakami, H., Hosoyama, A., Mizutani-Ui, Y., Takahashi, N. K., Sawano, T., Inoue, R.-i., Kaito, C., Sekimizu, K., Hirakawa, H., Kuhara, S., Goto, S., Yabuzaki, J., Kanehisa, M., Yamashita, A., Oshima, K., Furuya, K., Yoshino, C., Shiba, T., Hattori, M., Ogasawara, N., Hayashi, H., and Hiramatsu, K. (2001) Whole genome sequencing of meticillin-resistant *Staphylococcus aureus*. *Lancet 357*, 1225–1240.
13. Kunst, F., Ogasawara, N., Moszer, I., Albertini, A. M., Alloni, G., Azevedo, V., Bertero, M. G., Bessieres, P., Bolotin, A., Borchert, S., Borriss, R., Boursier, L., Brans, A., Braun, M., Brignell, S. C., Bron, S., Brouillet, S., Bruschi, C. V., Caldwell, B., Capuano, V., Carter, N. M., Choi, S. K., Codani, J. J., Connerton, I. F., Cummings, N. J., Daniel, R. A., Denizot, F., Devine, K. M., Dusterhoft, A., Ehrlich, S. D., Emmerson, P. T., Entian, K. D., Errington, J., Fabret, C., Ferrari, E., Foulger, D., Fritz, C., Fujita, M., Fujita, Y., Fuma, S., Galizzi, A., Galleron, N., Ghim, S. Y., Glaser, P., Goffeau, A., Golightly, E. J., Grandi, G., Guiseppi, G., Guy, B. J., Haga, K., Haiech, J., Harwood, C. R., Henaut, A., Hilbert, H., Holsappel, S., Hosono, S., Hullo, M. F., Itaya, M., Jones, L., Joris, B., Karamata, D., Kasahara, Y., Klaerr-Blanchard, M., Klein, C., Kobayashi, Y., Koetter, P., Koningstein, G., Krogh, S., Kumano, M., Kurita, K., Lapidus, A., Lardinois, S., Lauber, J., Lazarevic, V., Lee, S. M., Levine, A., Liu, H., Masuda, S., Mauel, C., Medigue, C., Medina, N., Mellado, R. P., Mizuno, M., Moestl, D., Nakai, S., Noback, M., Noone, D., O'Reilly, M., Ogawa, K., Ogiwara, A., Oudega, B., Park, S. H., Parro, V., Pohl, T. M., Portetelle, D., Porwollik, S., Prescott, A. M., Presecan, E., Pujic, P., and Purnelle, B.; et al. (1997) The complete genome sequence of the Gram-positive bacterium *Bacillus subtilis*. *Nature 390*, 249–256.
14. Takami, H., Nakasone, K., Takaki, Y., Maeno, G., Sasaki, R., Masui, N., Fuji, F., Hirama, C., Nakamura, Y., Ogasawara, N., Kuhara, S., and Horikoshi, K. (2000) Complete genome sequence of the alkaliphilic bacterium *Bacillus halodurans* and genomic sequence comparison with *Bacillus subtilis*. *Nucleic Acids Res. 28*, 4317–4331.
15. Takami, H., Takaki, Y., and Uchiyama, I. (2002) Genome sequence of *Oceanobacillus iheyensis* isolated from the Iheya Ridge and its unexpected adaptive capabilities to extreme environments. *Nucleic Acids Res. 30*, 3927–3935.
16. Johnson, E. G., Sparks, J. P., Dzikovski, B., Crane, B. R., Gibson, D. M., and Loria, R. (2008) Plant-pathogenic *Streptomyces* species produce nitric oxide synthase-derived nitric oxide in response to host signals. *Chem. Biol. 15*, 43–50.
17. Shatalin, K., Gusarov, I., Avetissova, E., Shatalina, Y., McQuade, L. E., Lippard, S. J., and Nudler, E. (2008) *Bacillus anthracis*-derived nitric oxide is essential for pathogen virulence and survival in macrophages. *Proc. Natl. Acad. Sci. U.S.A. 105*, 1009–1013.
18. Brown, G. M. (1985) Biosynthesis of pterins, in *Folates and Pterins* (Blakley, R. L., and Benkovic, S. J., Eds.) pp 115−154, John Wiley & Sons, New York.
19. Thony, B., Auerbach, G., and Blau, N. (2000) Tetrahydrobiopterin biosynthesis, regeneration and functions. *Biochem. J. 347*, 1–16.
20. Adak, S., Aulak, K. S., and Stuehr, D. J. (2002) Direct evidence for nitric oxide production by a nitric-oxide synthase-like protein from *Bacillus subtilis*. *J. Biol. Chem. 277*, 16167–16171.
21. Battista, J. R. (1997) Against all odds: The survival strategies of *Deinococcus radiodurans*. *Annu. Rev. Microbiol. 51*, 203–224.
22. Adak, S., Bilwes, A. M., Panda, K., Hosfield, D., Aulak, K. S., McDonald, J. F., Tainer, J. A., Getzoff, E. D., Crane, B. R., and Stuehr, D. J. (2002) Cloning, expression, and characterization of a nitric oxide synthase protein from *Deinococcus radiodurans*. *Proc. Natl. Acad. Sci. U.S.A. 99*, 107–112.
23. Buddha, M. R., Tao, T., Parry, R. J., and Crane, B. R. (2004) Regioselective nitration of tryptophan by a complex between bacterial nitric-oxide synthase and tryptophanyl-tRNA synthetase. *J. Biol. Chem. 279*, 49567–49570.
24. Kers, J. A., Wach, M. J., Krasnoff, S. B., Widom, J., Cameron, K. D., Bukhalid, R. A., Gibson, D. M., Crane, B. R., and Loria, R. (2004) Nitration of a peptide phytotoxin by bacterial nitric oxide synthase. *Nature 429*, 79–82.
25. Shiota, T. (1984) Biosynthesis of folate from pterin precursors, in *Folates and Pterins* (Blakley, R. L., and Benkovic, S. J., Eds.) pp 121−134, John Wiley & Sons, New York.
26. Blakley, R. L. (1984) Dihydrofolate reductase, in *Folates and Pterins* (Blakley, R. L., and Benkovic, S. J., Eds.) pp 191−253, John Wiley & Sons, New York.
27. Pant, K., Bilwes, A. M., Adak, S., Stuehr, D. J., and Crane, B. R. (2002) Structure of a nitric oxide synthase heme protein from *Bacillus subtilis*. *Biochemistry 41*, 11071–11079.
28. Blommel, P. G., and Fox, B. G. (2007) A combined approach to improving large-scale production of tobacco etch virus protease. *Protein Expression Purif. 55*, 53–68.
29. Pfleiderer, W. (1985) Chemistry of naturally occurring pterins, in *Folates and Pterins* (Blakley, R. L., and Benkovic, S. J., Eds.) pp 43−114, John Wiley & Sons, New York.
30. Zakrzewski, S. F., and Sansone, A. M. (1971) A new preparation of tetrahydrofolic acid. *Methods Enzymol. 18B*, 728–731.
31. Poe, M. (1977) Acidic dissociation constants of folic acid, dihydrofolic acid, and methotrexate. *J. Biol. Chem. 252*, 3724–3728.
32. Miles, E. W., Bauerle, R., Ahmed, S. A., and Seymour, K. (1987) Tryptophan synthase from *Escherichia coli* and *Salmonella typhimurium*. *Methods Enzymol. 142*, 398–414.

33. Vogel, H. J., and Bonner, D. M. (1956) Acetylornithinase of *Eschericia coli*: Partial purification and some properties. *J. Biol. Chem. 218*, 97–106.
34. Nelson, D. P., and Kiesow, L. A. (1972) Enthalpy of decomposition of hydrogen peroxide by catalase at 25° C (with molar extinction coefficients of H_2O_2 solutions in the UV). *Anal. Biochem. 49*, 474–478.
35. Clough, P. N., and Thrush, B. A. (1967) Mechanism of chemiluminescent reaction between nitric oxide and ozone. *Trans. Faraday Soc. 63*, 915–925.
36. Hevel, J. M., and Marletta, M. A. (1994) Nitric-oxide synthase assays, in *Methods in Enzymology*, p 250, Academic Press, New York.
37. Sligar, S. G. (1976) Coupling of spin, substrate, and redox equilibriums in cytochrome P450. *Biochemistry 15*, 5399–5406.
38. Klingenberg, M. (1958) Pigments of rat liver microsomes. *Arch. Biochem. Biophys. 75*, 376–386.
39. Omura, T., and Sato, R. (1964) The carbon monoxide-binding pigment of liver microsomes. I. Evidence for its hemoprotein nature. *J. Biol. Chem. 239*, 2370–2378.
40. Boggs, S., Huang, L., and Stuehr, D. J. (2000) Formation and reactions of the heme-dioxygen intermediate in the first and second steps of nitric oxide synthesis as studied by stopped-flow spectroscopy under single-turnover conditions. *Biochemistry 39*, 2332–2339.
41. Rusche, K. M., Spiering, M. M., and Marletta, M. A. (1998) Reactions catalyzed by tetrahydrobiopterin-free nitric oxide synthase. *Biochemistry 37*, 15503–15512.
42. Tommos, C., Skalicky, J. J., Pilloud, D. L., Wand, A. J., and Dutton, P. L. (1999) De novo proteins as models of radical enzymes. *Biochemistry 38*, 9495–9507.
43. Koppenol, W. H. (2007) Oxygen activation by cytochrome P450: A thermodynamic analysis. *J. Am. Chem. Soc. 129*, 9686–9690.
44. Hurshman, A. R., Krebs, C., Edmondson, D. E., and Marletta, M. A. (2003) Ability of tetrahydrobiopterin analogues to support catalysis by inducible nitric oxide synthase: Formation of a pterin radical is required for enzyme activity. *Biochemistry 42*, 13287–13303.
45. Wang, Z.-Q., Wei, C.-C., and Stuehr, D. J. (2002) A conserved tryptophan 457 modulates the kinetics and extent of N-hydroxy-L-arginine oxidation by inducible nitric-oxide synthase. *J. Biol. Chem. 277*, 12830–12837.
46. Fox, J. T., and Stover, P. J. (2008) Chapter 1: Folate-mediated one-carbon metabolism, in *Vitamins and Hormones* (Litwack, G., Ed.) pp 1−44, Academic Press, New York.
47. Wei, C.-C., Wang, Z.-Q., Wang, Q., Meade, A. L., Hemann, C., Hille, R., and Stuehr, D. J. (2001) Rapid kinetic studies link tetrahydrobiopterin radical formation to heme-dioxy reduction and arginine hydroxylation in inducible nitric-oxide synthase. *J. Biol. Chem. 276*, 315–319.